Wood Science and Technology (2021) 55:1109–1122
https://doi.org/10.1007/s00226-021-01308-3

ORIGINAL

TiO_2-carbonized medium-density fiberboard for the photodegradation of methylene blue

Justin Alfred Pe III[1] · Sung Phil Mun[1] · Min Lee[2]

Received: 27 November 2020 / Accepted: 2 June 2021 / Published online: 16 June 2021

Abstract

TiO_2-carbonized medium-density fiberboard (TiO_2-cMDF), prepared by carbonization of MDF treated with 50% (v/v) titanium tetraisopropoxide (Ti-tip) in isopropyl alcohol (IPA) as a precursor, was investigated for adsorption and photodegradation in aqueous methylene blue (MB) solution under UV-C (254 nm) irradiation. After full adsorption of MB, four successive cycles of photodegradation were conducted. After the second cycle, the TiO_2-cMDF was rinsed with water, dried, and subjected to photodegradation again. For every photodegradation cycle, the TiO_2-cMDF practically removed MB. The photodegradation results of the second (unrinsed) and third (rinsed) cycle were similar, however, the result of the fourth (rinsed) cycle was lower than the third cycle. The rate constant of adsorption was 3.3×10^{-3}/h and followed pseudo-first-order kinetics. The rate constant of photodegradation decreased from 11.0×10^{-3}/h (first cycle) to 5.9×10^{-3}/h (fourth cycle) and likewise followed pseudo-first-order kinetics. A reduction in Ti content on the surface of TiO_2-cMDF was observed after photodegradation based on scanning electron microscope-energy dispersive X-ray spectrometer (SEM–EDS) analysis; nonetheless, photodegradation of MB was still accomplished. Although TiO_2-cMDF in aqueous system exhibited slow photodegradation, it is due to the limited number of TiO_2-cMDF slabs. The number of slabs must be increased to improve the photocatalytic performance.

Introduction

Wood-based composites are materials used for nonstructural and structural applications encompassing furniture components, structural support in infrastructures, and panels for both overlay and underlay uses (Cai and Ross 2010). Wood-based composites, produced from processing raw wood, include plywood, glue-laminated timbers,

✉ Sung Phil Mun
msp@jbnu.ac.kr

[1] Department of Wood Science and Technology, Jeonbuk National University, Jeonju, Korea

[2] Department of Wood Products, National Institute of Forest Science, Seoul, Korea

particleboards, oriented strand boards, and fiberboards (low-, medium-, and high-density). Among these composites, medium-density fiberboards (MDFs) are manufactured wood-based panels with various physical properties and dimensions that can be tuned to specific MDF properties and density. To obtain enhanced performance properties of these wood-based materials, special re-purposed wood composites such as water-repellent composites, fire-retardant composites, and preservative-treated composites were produced (Stark et al. 2010). In addition to the arsenal of specialty wood composites were titanium dioxide (TiO_2) photocatalyst-treated composites. Recently, woody composites (Doi et al. 2000), delignified wood (He et al. 2019), wood templates (Liu et al. 2020), MDF (Giampiccolo et al. 2016), MDF biochar (Silvestri et al. 2019), and carbonized MDF (Lee et al. 2019a) were selected as support materials for TiO_2.

TiO_2 has gained significant attention as a photocatalyst based on its appreciable photocatalytic oxidation performance for the degradation of environmentally hazardous materials. TiO_2 has three main crystalline forms – anatase, rutile, and brookite. Among these, anatase TiO_2 demonstrated higher photocatalytic activity than rutile and brookite since anatase exhibited longer lifetime of photoexcited electrons and holes (Zhang et al. 2014). In addition, anatase showed better photocatalytic activity compared to other TiO_2 polymorphs in methylene blue (MB) photocatalytic oxidation (Chen et al. 2015). Photocatalytic studies were performed on MB, a cationic thiazine dye, since MB was the preferred test dye for the determination of the surface area of porous carbon materials (Nunes and Guerreiro 2011) and assessment of the activities of photocatalytic films (Mills 2012). TiO_2 suspensions have been used as a photocatalyst (Lakshmi et al. 1995; Zhang et al. 2008; Yao and Wang 2010) and required several separation processes to remove the TiO_2 slurry after the treatment (Kagaya et al. 1999). TiO_2 immobilization eliminates this complication and various supports for TiO_2 immobilization were reported (Alhaji et al. 2017).

MDFs are used as underlay board products due to their appearance and texture. In this regard, Kercher and Nagle (2002) presented an alternative utilization of MDFs through carbonization at high temperatures (600–1400 °C) for electrical applications. Park et al. (2009) manufactured large-sized crack-free cMDFs through a pressing carbonization method. Mun and Park (2011) improved the functionality of cMDF by carbonizing along with TiO_2 photocatalyst intended to simultaneously adsorb and degrade volatile organic compounds (VOCs). Recently, the photocatalytic activity of TiO_2-cMDF against VOCs such as toluene and formaldehyde was studied by Lee et al. (2019a, b). However, no studies were reported regarding the photocatalytic activity of the developed TiO_2-cMDF in aqueous solution. The purpose of this study was to investigate the adsorption and photodegradation of aqueous MB solution with TiO_2-cMDF under UV-C (254 nm) irradiation for future applications in water treatment.

Experimental

Preparation of TiO_2-cMDF

TiO_2-cMDF panel was previously prepared by Lee et al. (2019b) and the preparation was as follows. MDF with dimensions 260 mm (L) × 130 mm (W) × 12 mm (T)

(0.64 g/cm^2, E1 grade, Sunchang Industry, Korea) was evenly treated with a photocatalyst precursor Ti-tip (CAS 546–68-9) (98%, Daejung Chemicals, Korea) diluted in 50% (v/v) IPA (CAS 67–63-0) (99.5%, Daejung Chemicals, Korea) via brush coating method. An amount of 7.21 g of 50% Ti-tip was applied to the MDF surface. Afterward, the solvent was volatilized under a hood at room temperature and the Ti-tip treated MDFs were dried in a convection oven at 60 °C for 3 h. The dried Ti-tip treated MDFs were then carbonized in an electric furnace with a ramping rate of 50 °C/h to 700 °C and held for 2 h.

Crystallinity of TiO_2-cMDF

The TiO_2 crystalline structure on the surface of TiO_2-cMDF was characterized by X-ray diffraction (XRD, D/Max-2500, Rigaku, Japan). After carbonization at 700 °C, a portion of TiO_2-cMDF surface was analyzed under the conditions of 40 kV and 30 mA in the range of 5–80° from the starting angle. A portion of the surface of a cMDF carbonized at 800 °C was measured for comparison purposes. All spectra were normalized and used.

Evaluation of adsorption and photodegradation of MB

The TiO_2-cMDF panel with dimensions 200 mm (L) × 100 mm (W) × 7 mm (T) prepared from abovementioned method was cut into slabs with dimensions 60 mm (L) × 20 mm (W) × 3 mm (T). Four slabs were secured on a fabricated stainless-steel frame using a polyethylene hot-melt adhesive. The TiO_2-cMDF slabs attached to a fabricated stainless-steel frame were immersed in 475 mL of 10.0 ppm MB (CAS 61–73-4) (95%, Yakuri Pure Chemicals, Japan) solution in a 500-mL glass reactor under stirring (Eyela RCN-7, Japan) for the adsorption experiment. After adsorption, the solution was discarded and fresh 475 mL of 10.0 ppm MB solution was added, and then a UV-C (254 nm, 4.0 mW/cm^2) (Magisam, Korea) light source was inserted into the fabricated stainless-steel frame. The representation of the system employed for adsorption and photodegradation is shown in Fig. 1.

The photodegradation of MB was performed for four cycles. The MB solution after each cycle of photodegradation was discarded and fresh 475 mL of 10.0 ppm MB solution was added. After the second cycle, the TiO_2-cMDF was rinsed with distilled deionized (DI) water, dried in a convection oven at 65 °C overnight, and then subjected to the next cycle of photodegradation. Since the UV-C light source generated heat during the experiment, the water lost due to evaporation was replenished periodically. The removal of MB was determined by the decrease in absorbance at 665 nm using a UV–Vis spectrophotometer (Optizen 3220, Korea). The %MB removal was calculated using the following equation:

$$\%\text{MBremoval} = \frac{C_o - C_t}{C_o} \times 100 \quad (1)$$

where C_o is initial concentration (mg/L) and C_t is concentration at time t. The non-linear plots of the %MB removal were transformed to linear plots using either

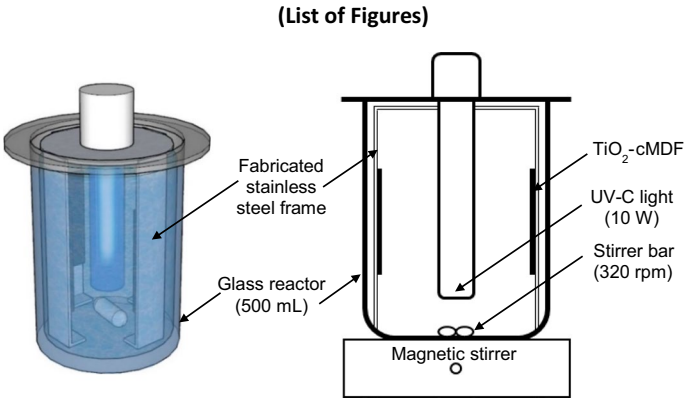

Fig. 1 Representation of the system for adsorption and photodegradation

semi-log normalization for pseudo-first-order kinetics or inverse normalization for pseudo-second-order kinetics to estimate the rate constant of the photodegradation cycle using the following equations:

$$\ln C_t = \ln C_o - kt \tag{2}$$

$$\frac{1}{C_t} = \frac{1}{C_o} + kt \tag{3}$$

where k is rate constant (1/h) and t is time (h).

Surface morphology, Ti distribution, and Ti layer thickness of TiO_2-cMDF

The untreated TiO_2-cMDF and TiO_2-cMDF after photodegradation were subjected to surface analysis. Surface morphology and the determination of Ti distribution, elemental analysis, and Ti layer thickness were conducted using SEM–EDS (SUPRA 40VP, Zeiss, Germany) at the Center for University-wide Research Facility, Jeonbuk National University (JBNU). Surface images were taken under 350× magnification and four data points were collected for elemental analysis. Cross-sectional images of TiO_2-cMDF were done under 40× magnification.

Results and discussion

Specialty wood composites such as cMDFs and TiO_2-cMDFs were prepared through a pressing carbonization method to produce a smooth, crack-free, and twist-free carbonized fiberboard (Fig. 2) (Park et al. 2009). Fiberboard characteristics of cMDFs and TiO_2-cMDFs such as shrinkage and weight reductions at various carbonization temperatures were already reported (Lee et al. 2019a). After carbonization at 700 °C, the length and width of TiO_2-cMDF decreased to about 20% and the weight

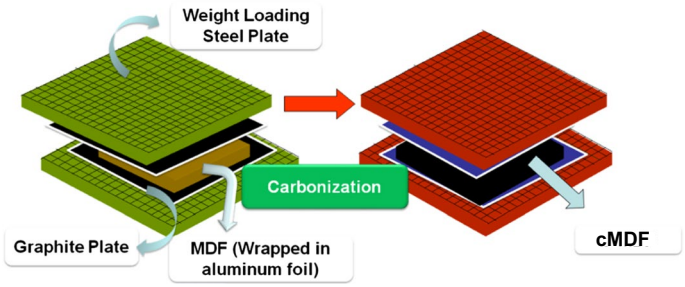

Fig. 2 Pressing carbonization method for manufacturing cMDF

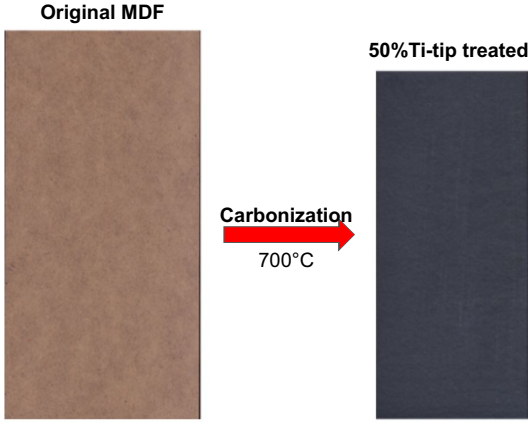

Fig. 3 Appearance of original MDF and TiO_2-cMDF

dropped down to 70% from the original weight of MDF. The original MDF and TiO_2-cMDF are shown in Fig. 3.

Crystallinity of TiO_2-cMDF

The formation of anatase crystals on the surface of cMDF was sought for the preparation of TiO_2-cMDF. The work of Lee et al. (2019b) showed that at carbonization temperatures of 600–900 °C, anatase was the favored TiO_2 crystalline structure on the surface of cMDF and carbonization beyond these temperatures revealed increased amounts of rutile. Figure 4 shows the XRD spectra of TiO_2-cMDF carbonized at 700 °C for 2 h in comparison to cMDF carbonized at 800 °C for 2 h (Lee et al. 2019b). For cMDF carbonized at 800 °C, two broad peaks at 24° and 43° appeared in the XRD spectrum. These peaks are a result of ultrastructural changes in wood charcoal toward graphitization (Kumar et al. 1993; Nishimiya et al. 1998). In the case of TiO_2-cMDF, the XRD peaks indicated that anatase-type TiO_2 was successfully formed on the cMDF during the carbonization at 700 °C. The XRD pattern for TiO_2-cMDF is in good agreement with characteristic peaks of anatase-type

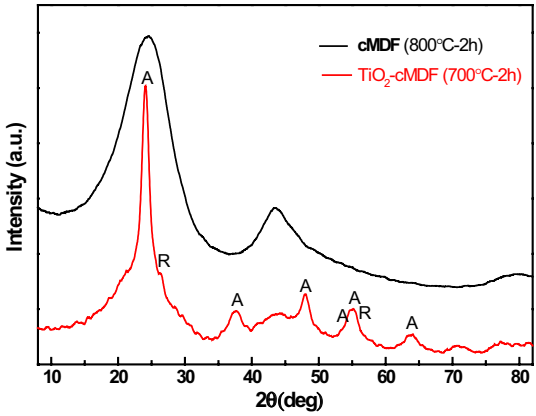

Fig. 4 X-ray diffractograms of cMDF and TiO_2-cMDF

TiO_2 at 2θ values of 24.8°, 37.3°, 47.6°, 53.5°, 55.1°, and 62.2° (JCPDS Card no. 21-1272).

Adsorption characteristics of MB on TiO_2-cMDF

In general, carbonized materials such as wood charcoal are microporous and can adsorb low molecular weight VOCs such as formaldehyde (Lee et al. 2007) and toluene (Singh et al. 2010). Activated cMDFs exhibited specific surface areas ranging from 400–1000 m^2/g (Kercher and Nagle 2003) while TiO_2-cMDFs range from 100–500 m^2/g (Mun and Park 2011). Considering the abilities of carbonized materials to adsorb organic compounds, TiO_2-cMDF was treated with MB solution to achieve a full adsorption cycle. The adsorption of MB on TiO_2-cMDF was almost completed in 852 h (Fig. 5a) and followed pseudo-first-order kinetics (Fig. 5b).

MB photodegradation performance of TiO_2-cMDF

Photodegradation was performed for four cycles, of which the third and fourth cycles were carried out differently from the first and second cycle. After the second cycle, the TiO_2-cMDF was rinsed with water, dried, and subjected to photodegradation again. The kinetics results of the photodegradation cycles are shown in Fig. 6 and tabulated in Table 1.

Photodegradation in the first and second cycle occurred at 348 h and 420 h with attainment of 99% removal of MB, respectively (Fig. 6a). As expected, the MB removal by photodegradation was much faster than adsorption due to photocatalytic oxidation of MB. Figure 7 shows a possible mechanism for the photodegradation of MB using TiO_2-cMDF based on well-established mechanisms (Lakshmi et al. 1995; Mills and Wang 1999; Houas et al. 2001; Xu et al. 2014). When the bandgap energy of TiO_2 anatase ($E_g = 3.2$ eV) is stimulated with a UV (254 nm, 4.8 eV) light source, the electrons from the valence band will be excited to the conduction band thereby generating holes (h^+) and electrons (e^-). These h^+ and e^- produce hydroxyl radicals,

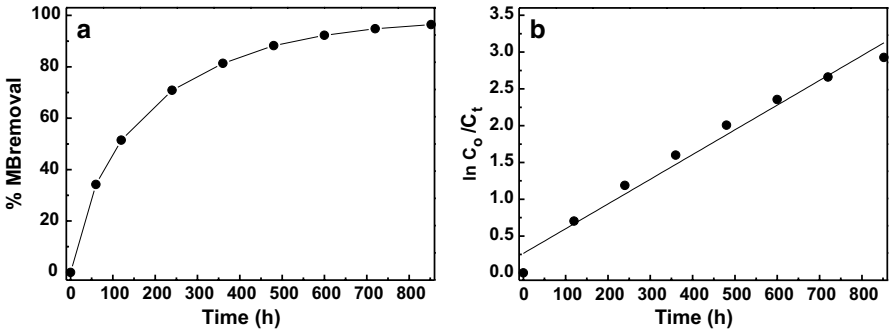

Fig. 5 Adsorption kinetics of MB **a** %MB removal and **b** Normalized plot

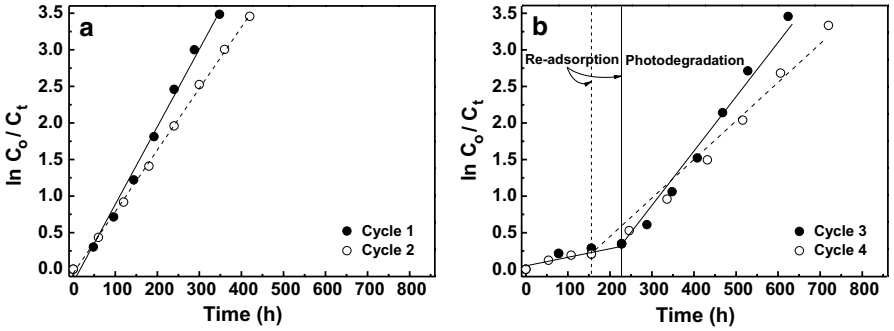

Fig. 6 Photodegradation kinetics of MB **a** Cycles 1–2: without rinsing, **b** Cycles 3–4: with rinsing

Table 1 Kinetics of MB removal through adsorption and photodegradation using TiO_2-cMDF

Phase		Cycle	Rate constant ($\times 10^{-3}$/h)	t_{99}, h (days)
Adsorption		–	3.3	852 (35.5)
Photodegradation	w/o rinsing	1	11.0	348 (14.5)
		2	8.6	420 (17.5)
	w/ rinsing	3	8.8	624 (26.0)
		4	5.9	720 (30.0)

obtained from the interaction of water and the superoxide radical anion, which have sufficient energy to degrade MB. Degradation of MB was confirmed by the decrease in the intensity of visible absorption at maximum wavelength (665 nm), as shown in Fig. 8. In addition, the changes in spectral absorption recorded for the first cycle showed a hypsochromic shift (λ_{max} shifting to a shorter wavelength) which can be attributed to the demethylation of MB (Zhang et al. 2001; Yogi et al. 2008) and reduction in conjugation through the breakdown of the chromophores that led to the degradation of the molecule.

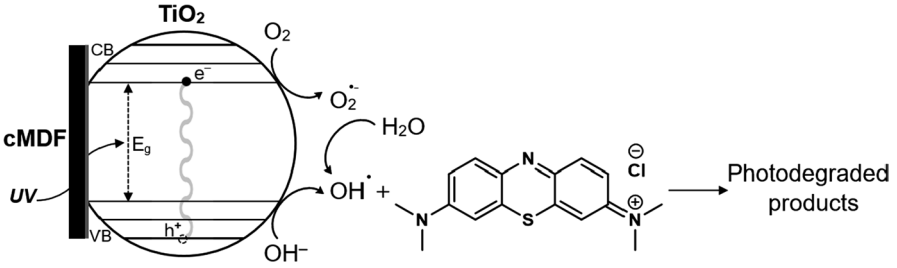

Fig. 7 Possible mechanism for the photodegradation of MB

Photodegradation, like adsorption as mentioned above, followed pseudo-first-order kinetics and was in agreement with early work by Matthews (1989) on the photodegradation of MB via TiO_2 photocatalysis. The rate constant appeared to be 11.0×10^{-3}/h for the first cycle and 8.6×10^{-3}/h for the second cycle. Rate constant of the second cycle decreased by 22% compared to the first cycle. The decreased accessibility to the effective Ti surface may have caused this result. The existing MB layer on the TiO_2-cMDF surface (Fig. 9b) and additional undecomposed MB that saturated the TiO_2-cMDF surface (Fig. 9c) might have hindered the photodegradation process.

For this reason, after the second cycle, the TiO_2-cMDF was rinsed with DI water to wash off some adhered MB (Fig. 9d) and then dried. TiO_2-cMDF was subjected to a process of brief re-adsorption and confirmed that rinsing removed some adhered MB, since 30% of MB from the fresh solution was removed via re-adsorption. Upon reaching equilibrium at 228 h, the UV-C (254 nm) light was turned on. Photodegradation in the third cycle proceeded for further 396 h to attain 99% removal of MB (Fig. 6b). The rate constant of the third cycle was 8.8×10^{-3}/h and was similar to the rate constant of the second cycle.

After the third cycle, the TiO_2-cMDF was rinsed and subjected to re-adsorption. About 20% of MB was removed by re-adsorption and upon reaching equilibrium at 156 h, the UV-C light was turned on. However, when the TiO_2-cMDF was rinsed

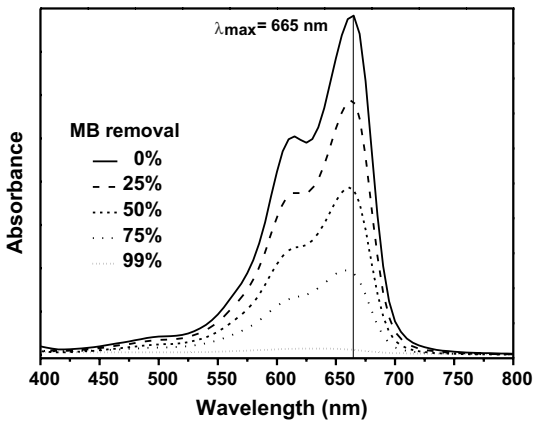

Fig. 8 Changes in spectral absorption of MB solution (similar to all photodegradation cycles)

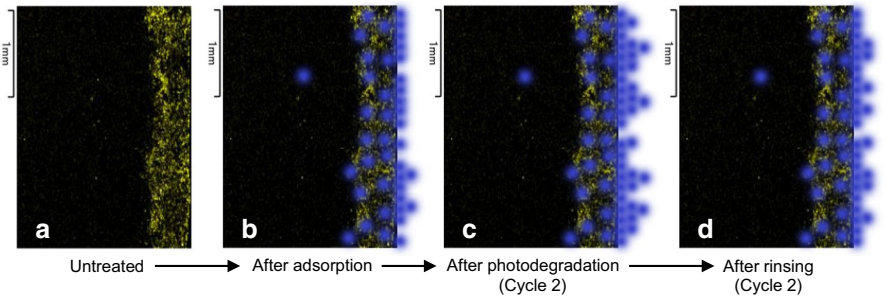

Fig. 9 Schematic illustration of the TiO_2-cMDF surface after adsorption, photodegradation, and rinsing

after the third cycle, the rate constant of the fourth cycle decreased by 33% compared to the third cycle. This indicates that the rinsing after the third cycle was less effective for the removal of adhered MB. A plausible reason for the removal of effective TiO_2 was that TiO_2-cMDF was immersed in an aqueous medium for the whole experimental period and also rinsed after the third cycle. Thus, ion distribution and elemental analysis by SEM–EDS were performed on TiO_2-cMDF cross section and surface to estimate the effective Ti distribution and content.

The cross-sectional SEM and ion distribution images of untreated TiO_2-cMDF are shown in Fig. 10. The Ti layer was found to be 0.4 mm thick, which is 20% of the 2.0 mm thick slab; this finding suggests that Ti layer thickness would have sufficient surface for photocatalytic activity. The surface SEM image after four photodegradation cycles is shown in Fig. 11. Results of elemental analysis by EDS indicated that Ti was significantly removed during the series of photodegradation (Fig. 12, Table 2). Although the Ti content was reduced on the surface of TiO_2-cMDF, photodegradation of MB was still accomplished since there were still effective Ti dispersed on the surface of TiO_2-cMDF after photodegradation (Fig. 13b). In addition, the ion distribution for untreated TiO_2-cMDF surface (Fig. 13c) did not contain Cl which originated from MB, but after photodegradation, Cl adhered to the surface (Fig. 13d) as well. This indicates that Cl along with undecomposed MB may block the effective TiO_2 surface causing decreased photodegradation rate constants.

Table 3 shows related literatures on TiO_2-treated wood and wood-based composites. Immobilization of TiO_2 in wood and wood-based materials through several methods (i.e., sol–gel, hydrothermal, coating, etc.) were prepared for water repellency (Chu et al. 2014; Pori et al. 2016; Zanatta et al. 2017), protection from UV and

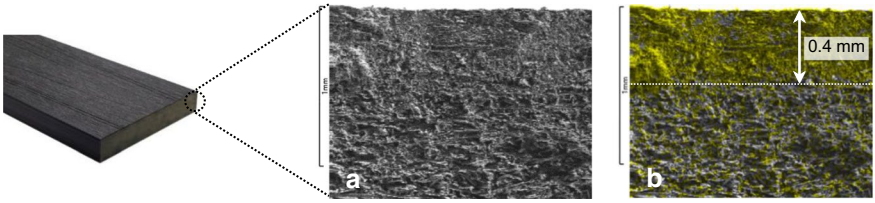

Fig. 10 Cross-sectional **a** SEM image and **b** Ti layer (yellow color) distribution of untreated TiO_2-cMDF

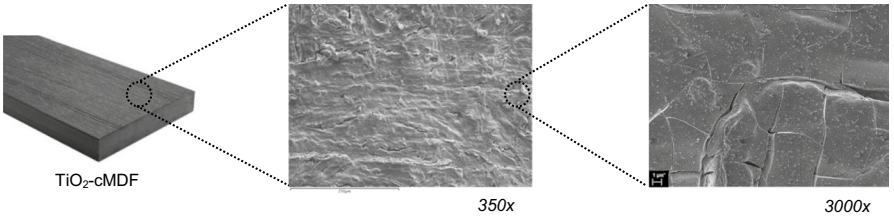

Fig. 11 Surface SEM images of TiO_2-cMDF after four photodegradation cycles

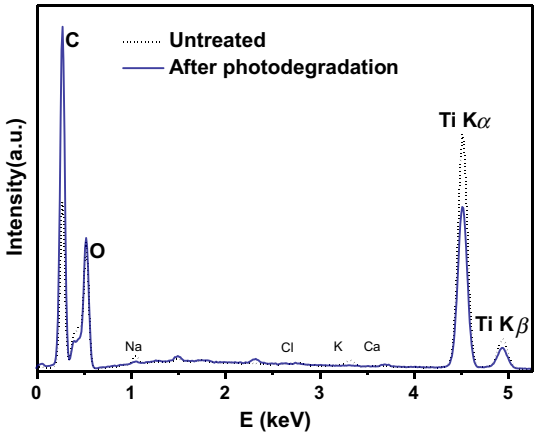

Fig. 12 EDX spectra of TiO_2-cMDF surface: untreated and after photodegradation

Table 2 Atomic percentage of TiO_2-cMDF surface: untreated and after photodegradation

Element	Atomic percentage	
	Untreated	After photodegradation
C	38.00	69.52
O	37.46	20.87
Ti	23.26	9.30

moisture (Rassam et al. 2012; Jnido et al. 2019), and removal of VOCs (Doi et al. 2000; Lee et al. 2019a,b; Liu et al. 2020) and organic dyes (Sun et al. 2013; He et al. 2019; Silvestri et al. 2019). Nasr et al. (2018) did a comprehensive review on photocatalytic processes, reaction mechanisms, and photocatalytic applications related to TiO_2. Sun et al. (2013) developed a TiO_2-treated wood template suspension to remove Rhodamine B. An interesting TiO_2-decorated bleached wood support that floats and removed MB under ambient sunlight was prepared by He et al. (2019). Silvestri et al. (2019) re-processed MDF residue into MDF biochar and efficiently removed MB.

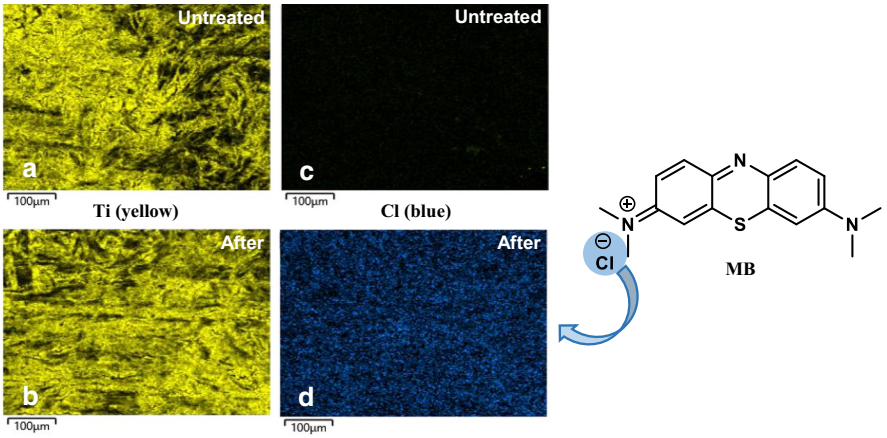

Fig. 13 Surface Ti & Cl distribution images of TiO_2-cMDF: untreated and after photodegradation

Table 3 Summary of TiO_2-treated wood and wood-based composites with their applications

Support	Applications	Efficiency	Method	References
Wood (*Acacia* sp.)	Wood hydrophobicity	–	Pressure/Hydrothermal	Chu et al. (2014)
Wood (*Picea* sp.)	Wood hydrophobicity	–	Hydrothermal	Pori et al. (2016)
Wood (*Pinus* sp.)	Wood hydrophobicity	–	Microwave solvothermal	Zanatta et al. (2017)
Wood (*Fagus* sp.)	UV and moisture protection	–	Sol–gel	Rassam et al. (2012)
Wood (*Fagus* sp.)	UV and moisture protection	–	Atm. pressure plasma jet	Jnido et al. (2019)
Wood (*Thuja* sp.)	Formaldehyde removal	75%, 7 h	Sol–gel	Doi et al. (2000)
cMDF	Formaldehyde & toluene removal	99%, 8 h	Sol–gel	Lee et al. (2019a,b)
Wood templates	Formaldehyde removal	20%, 5 h	Hydrothermal	Liu et al. (2020)
Wood template	Rhodamine B removal	90%, 3 h	Sol–gel	Sun et al. (2013)
Bleached wood	MB removal	99%, 7 h	Coating	He et al. (2019)
MDF biochar	MB removal	86%, 3 h	Coating	Silvestri et al. (2019)
cMDF	MB removal	99%, 348 h	Sol–gel	This work

The photodegradation efficiency developed for this study was slow compared to other TiO_2 treated wood-based composites as there were a small number of TiO_2-cMDF slabs, which underwent a full cycle of adsorption prior to photodegradation. To increase the photocatalytic performance of TiO_2-cMDF, additional slabs must be incorporated.

Conclusion

The TiO_2-cMDF prepared by carbonization of MDF treated with Ti-tip as a precursor demonstrated removal of dye through adsorption of MB to the surface, photodegradation of MB in bulk solution, and photodegradation of adsorbed MB on the surface in the presence of a UV light source. This work is a preliminary study on the photocatalytic activity of TiO_2-cMDF in aqueous solutions. The TiO_2-cMDF could practically remove MB after several cycles of photodegradation although there was a decrease in the rate constant and reduction in Ti particles on the surface of the photocatalyst. The photodegradation under the system that was developed for this study was slow but nevertheless photodegradation occurred. To increase the photocatalytic performance of TiO_2-cMDF, the number of slabs must be increased. Consequently, the outcomes propose TiO_2-cMDF is a prospective biomaterial for wastewater treatment.

Acknowledgements The authors would like to thank Jung Tak Bae (College of Engineering Affiliated Facility, JBNU) for machining the stainless-steel frame and Kim Yu Jin (Wood Processing Support Center, JBNU) for precisely cutting the TiO_2-cMDF slabs.

Declarations

Conflict of interest The authors declare that they do not have any conflict of interest.

References

Alhaji MH, Sanaullah K, Khan A, Hamza A, Muhammad A, Ishola MS, Rigit ARH, Bhawani SA (2017) Recent developments in immobilizing titanium dioxide on supports for degradation of organic pollutants in wastewater- A review. Int J Environ Sci Technol 14(9):2039–2052

Cai Z, Ross RJ (2010) Mechanical properties of wood-based composite materials GTR-190. Wood handbook wood as an engineering material Chapter 12. USDA USFS FPL, Madison WI, pp 12–1

Chen WT, Chan A, Jovic V, Sun-Waterhouse D, Murai K, Idriss H, Waterhouse GIN (2015) Effect of TiO_2 crystallite size, TiO_2 polymorph and test conditions on the photo-oxidation rate of aqueous methylene blue. Top Catal 58:85–102

Chu T, Chuong PV, Tuong VM (2014) Wettability of wood pressure-treated with TiO_2 gel under hydrothermal conditions. BioResources 9(2):2396–2404

Doi M, Saka S, Miyafuji H, Goring DAI (2000) Development of carbonized TiO_2-woody composites for environmental cleaning. Mater Sci Res Int 6(1):15–21

Giampiccolo A, Ansell MP, Tobaldi DM, Ball RJ (2016) Synthesis of Co-TiO_2 nanostructured photocatalytic coatings for MDF substrates. Green Mater 4(4):140–149

He Y, Li H, Guo X, Zheng R (2019) Bleached wood supports for floatable, recyclable, and efficient three dimensional photocatalyst. Catalysts 9(2):115

Houas A, Lachheb H, Ksibi M, Elaloui E, Guillard C, Herrmann JM (2001) Photocatalytic degradation pathway of methylene blue in water. Appl Catal B 31(2):145–157

Jnido G, Ohms G, Viöl W (2019) Deposition of TiO_2 thin films on wood substrate by an air atmospheric pressure plasma jet. Coatings 9:441

Kagaya S, Shimizu K, Arai R, Hasegawa K (1999) Separation of titanium dioxide photocatalyst in its aqueous suspensions by coagulation with basic aluminum chloride. Water Res 33(7):1753–1755

Kercher AK, Nagle DC (2002) Evaluation of carbonized medium-density fiberboard for electrical applications. Carbon 40:1321–1330

Kercher AK, Nagle DC (2003) Monolithic activated carbon sheets from carbonized medium-density fiberboard. Carbon 41:3–13

Kumar M, Gupta RC, Sharma T (1993) X-ray diffraction studies of acacia and eucalyptus wood chars. J Mater Sci 28:805–810

Lakshmi S, Renganathan R, Fujita S (1995) Study on TiO_2-mediated photocatalytic degradation of methylene blue. J Photochem Photobio A Chem 88:163–167

Lee OK, Choi JW, Jo TS, Paik KH (2007) Adsorption of formaldehyde by wood charcoal-based building materials. Mokchae Gonghak 35(3):61–69

Lee M, Park SB, Mun SP (2019a) One-step preparation of TiO_2-carbonized medium density fiberboard for volatile organic compound degradation. BioResources 14(3):5533–5543

Lee M, Park SB, Mun SP (2019b) Synthesis of TiO_2 via modified sol-gel method and its use in carbonized medium density fiberboard for toluene decomposition. BioResources 14(3):6516–6528

Liu Y, Zhu X, Yaun D, Wang W, Gao L (2020) Preparation and characterization of TiO_2 based on wood templates. Sci Rep 10:12444

Matthews RW (1989) Photocatalytic oxidation and adsorption of methylene blue on thin films of near-ultraviolet-illuminated TiO_2. J Chem Soc, Faraday Trans 1 85(6):1291–1302

Mills A (2012) An overview of the methylene blue ISO test for assessing the activities of photocatalytic films. Appl Catal B 128:144–149

Mills A, Wang J (1999) Photobleaching of methylene blue sensitized by TiO_2: an ambiguous system? J Photochem Photobio A 127(1–3):123–134

Mun SP, Park SB (2011) Preparation of the functionality enhanced carbonized medium density fiberboard by pretreatment of photocatalytic precursor, titanium tetraisopropoxide. Abstracts of the Forest Products Society, 61st International Convention, Portland, p 127

Nasr M, Eid C, Habchi R, Miele P, Bechelany M (2018) Recent progress on titanium dioxide nanomaterials for photocatalytic applications. Chemsuschem 11:3023–3047

Nishimiya K, Hata T, Imamura Y, Ishihara S (1998) Analysis of chemical structure of wood charcoal by X-ray photoelectron spectroscopy. J Wood Sci 44:56–61

Nunes CA, Guerreiro MC (2011) Estimation of surface area and pore volume of activated carbons by methylene blue and iodine numbers. Quim Nova 34(3):472–476

Park SB, Lee SM, Park JY, Lee SH (2009) Manufacture of crack-free carbonized board from fiberboard. Mokchae Konghak 37(4):293–299

Pori P, Vilčnik A, Petrič M, Škapin AS, Mihelčič M, Vuk AS, Novak U, Orel B (2016) Structural studies of TiO_2/wood coatings prepared by hydrothermal deposition of rutile particles from $TiCl_4$ aqueous solutions of spruce (*Picea abies*) wood. Appl Surf Sci 375:125–138

Rassam G, Abdi Y, Abdi A (2012) Deposition of TiO_2 nano-particles on wood surfaces for UV and moisture protection. J Exp Nanosci 7(4):468–476

Silvestri S, Stefanello N, Sulkovski AA, Foletto EL (2019) Preparation of TiO_2-supported on MDF biochar for simultaneous removal of methylene blue by adsorption and photocatalysis. J Chem Technol Biotechnol 95(10):2723–2729

Singh K, Singh RS, Rai BN, Upadhyay SN (2010) Biofiltration of toluene using wood charcoal as the biofilter media. Bioresour Technol 101(11):3947–3951

Stark NM, Cai Z, Carll C (2010) Wood-based composite materials panel products glued-laminated timber, structural composite lumber, and wood-nonwood composite materials. GTR-190. Wood handbook wood as an engineering material Chapter 11. USDA USFS FPL, Madison WI, pp 11–12

Sun Q, Lu Y, Tu J, Yang D, Cao J, Li J (2013) Bulky macroporous TiO_2 photocatalyst with cellular structure via facile wood-template method. Int J Photoenergy. https://doi.org/10.1155/2013/649540

Xu C, Rangaiah GP, Zhao XS (2014) Photocatalytic degradation of methylene blue by titanium dioxide: Experimental and modeling study. Ind Eng Chem Res 53:14641–14649

Yao J, Wang C (2010) Decolorization of methylene blue with TiO_2 sol via UV irradiation photocatalytic degradation. Int J Photoenergy. https://doi.org/10.1155/2010/643182

Yogi C, Kojima K, Wada N, Tokumoto H, Takai T, Mizoguchi T, Tamiaki H (2008) Photocatalytic degradation of methylene blue by TiO_2 film and Au particles-TiO_2 composite film. Thin Solid Films 516(17):5881–5884

Zanatta P, Gallio E, Ribes DD, Lazarotto M, Gatto DA, Moreira ML (2017) The use of microwave system to deposit TiO_2 on wood surface to improve water repellency. Amaz J Plant Resear 1:39–44

Zhang T, Oyama T, Aoshima A, Hidaka H, Zhao J, Serpone N (2001) Photooxidative *N*-demethylation of methylene blue in aqueous TiO_2 dispersions under UV irradiation. J Photochem Photobio A 140(2):163–172

Zhang X, Wu F, Wu XW, Chen P, Deng N (2008) Photodegradation of acetaminophen in TiO_2 suspended solution. J Hazard Mater 157(2–3):300–307

Zhang J, Zhou P, Liu J, Yu J (2014) New understanding of the difference of photocatalytic activity among anatase, rutile, and brookite TiO_2. Phys Chem Chem Phys 16(38):20382–20386